Supplementary Figure S1

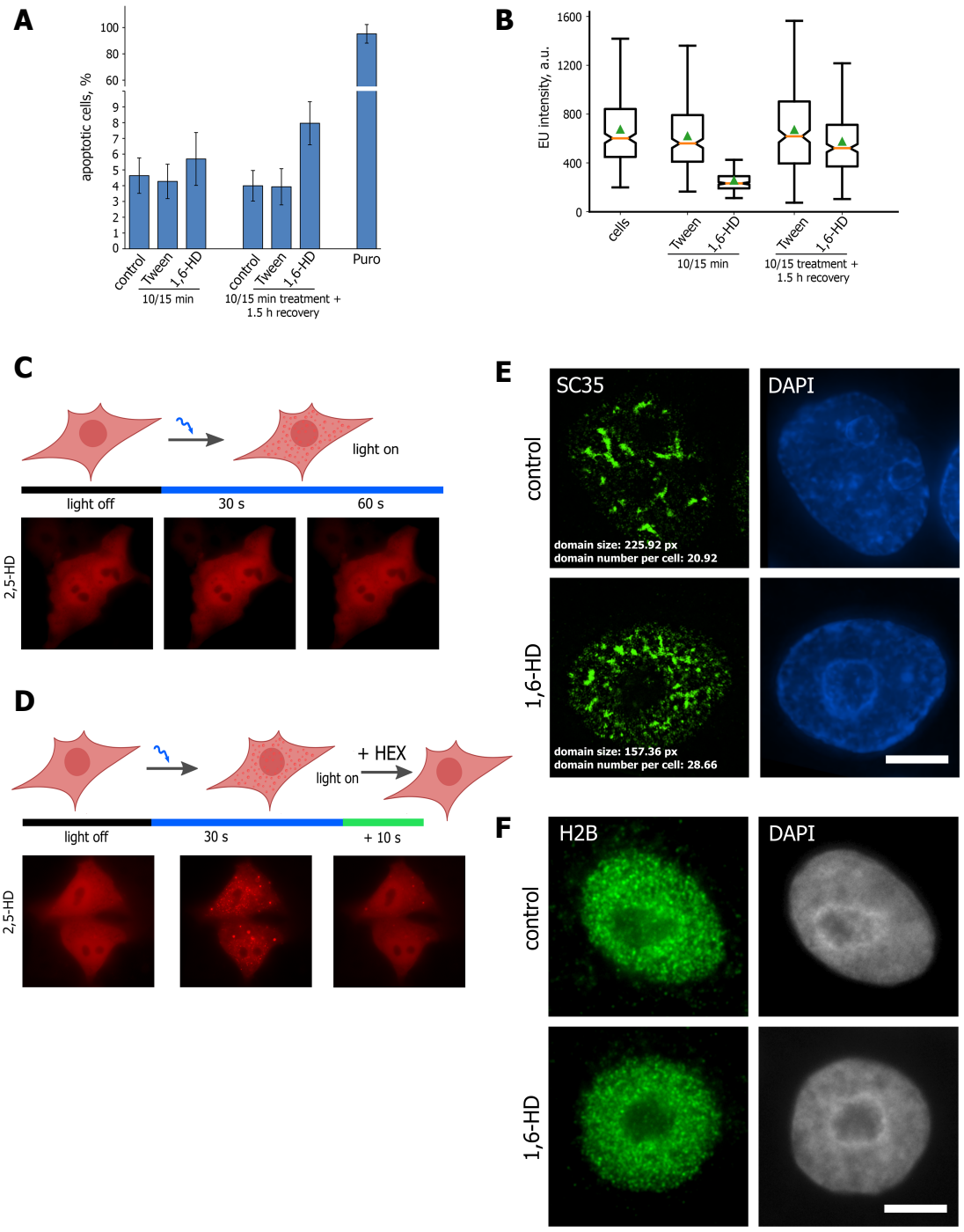

Supplementary Figure S1. 1,6-HD affects LLPS in living human cells. (**A**) HeLa cells were untreated or treated with Tween 20 (1%, 10 min; “Tween”), followed with 1,6-HD (5%, 15 min; “1,6-HD ”) before being analyzed using CellEvent Caspase 3/7 Detection Reagent. The cells treated as described and then incubated in fresh culture medium for 1.5 h were analysed as well. Percentage of caspase 3/7-positive (apoptotic) cells is shown. (**B**) HeLa cells treated as described in (A) were pulsed with 5-ethyniluridine (EU, 200 μM, 15 min). Box plots show the EU fluorescence intensities. Horizontal lines represent the medians. (**C**) HeLa cells transfected with pHT-FUSN-mCh-Cry2WT were transiently permeabilized with Tween 20 and treated with 2,5-HD (5%, 15 min). OptoDroplet formation was monitored as described in Shin et al., 2017. Accompanying untreated (control) and 1,6-HD-treated cells are shown in Fig. 1A. (**D**) HeLa cells transfected with pHT-FUSN-mCh-Cry2WT were light-illuminated to induce optoDroplet formation. Then 2,5-HD (5%) was added to the culture medium; optoDroplet existence was monitored after ten seconds of incubation with the drug. Accompanying 1,6-HD-treated cells are shown in Fig. 1B. (**E**) HeLa cells were first transiently permeabilized with Tween 20 and then were either left untreated (control) or treated with 1,6-HD (5%, 15 min) before being stained for SC35 (SRSF2). The DNA was stained with DAPI. The samples were analyzed by structured illumination microscopy (SIM). Nanodomain clustering analysis (see Methods for details) was performed (13 control cells and 9 1,6-HD-treated cells were analyzed). Average nanodomain cluster sizes and numbers of nanodomains per cell are depicted in each case. (**F**) HeLa cells treated as in (E) were stained for histone H2B and analyzed by epifluorescence microscopy. The DNA was stained with DAPI. Scale bar: 10 μm.

Supplementary Figure S2

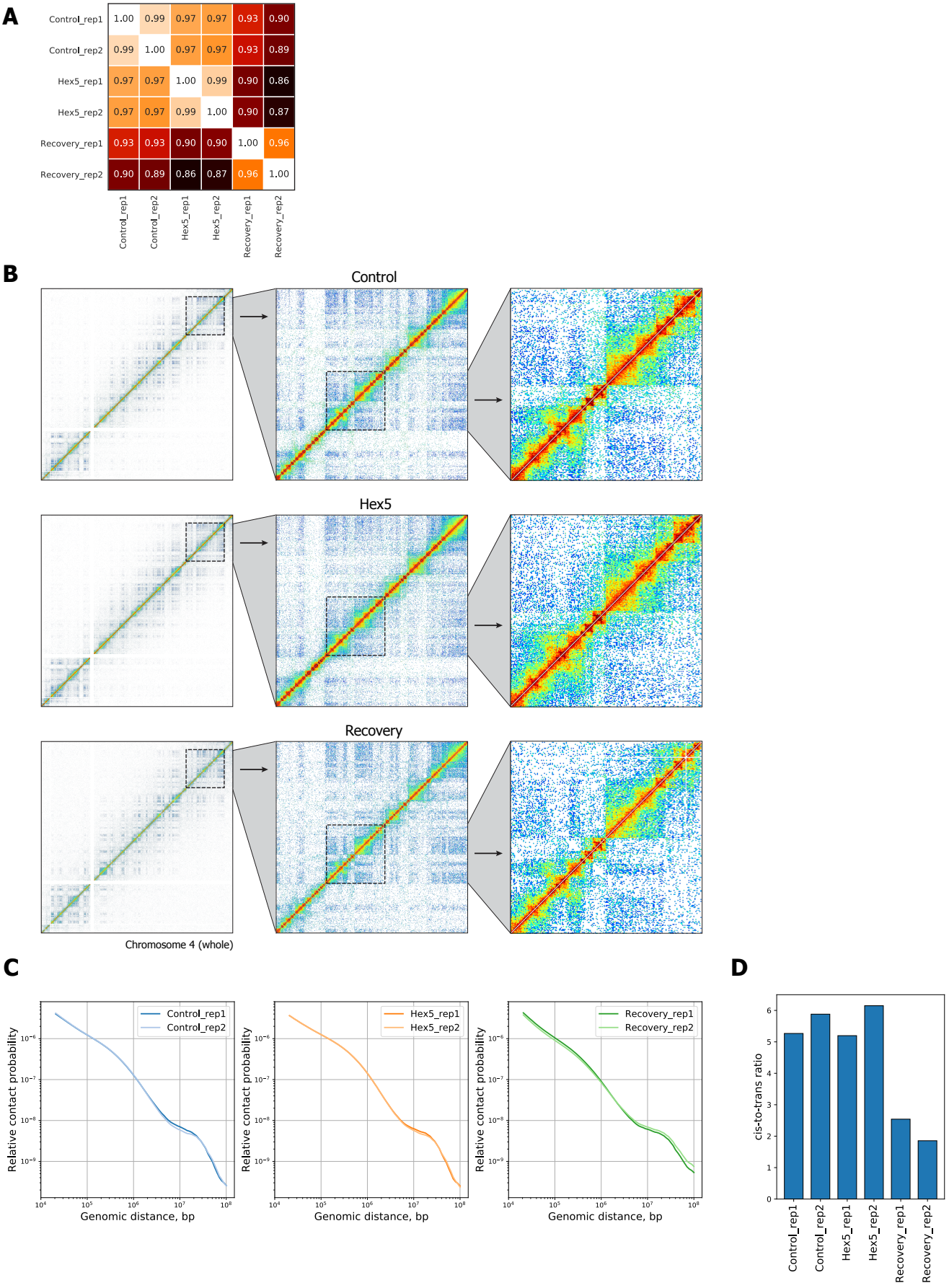

Supplementary Figure S2. Hi-C data processing. (**A**) Pearson's correlation coefficient between biological replicates of the Hi-C experiments. (**B**) Visualization of the Control, Hex5, and Recovery contact matrices at a 20-kb resolution. (**C**) Dependence of contact probability, $P_c(s)$, on genomic distance, s for the Control, Hex5, and Recovery biological replicates. (**D**) Ratio between cis (intrachromosomal) and trans (interchromosomal) contacts for the Control, Hex5, and Recovery biological replicates.

Supplementary Figure S3

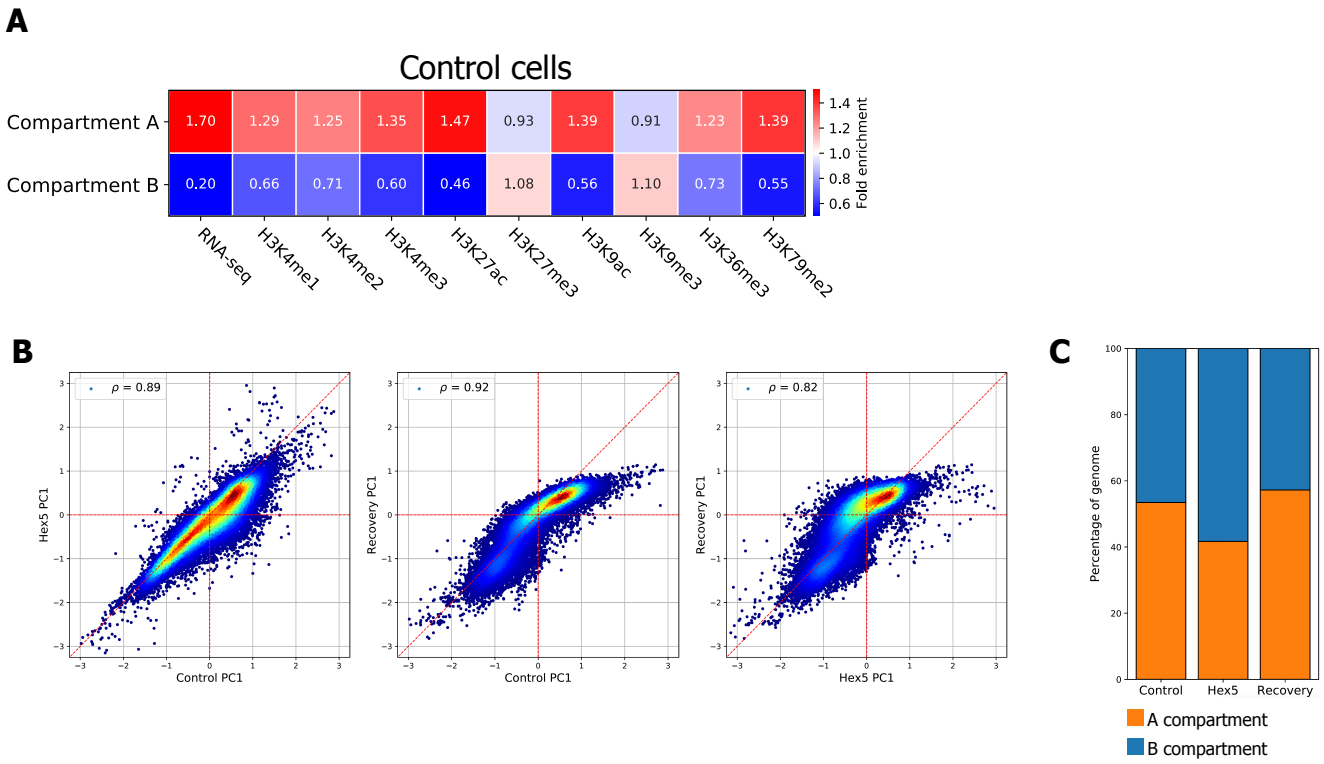

Supplementary Figure S3. Compartment annotation. (**A**) Enrichment of different epigenetic markers in the A and B compartments annotated in control cells. (**B**) Scatter plots showing the correlations among PC1 values for the Control, Hex5, and Recovery samples. (**C**) Coverage of the genome with A and B compartments.

Supplementary Figure S4

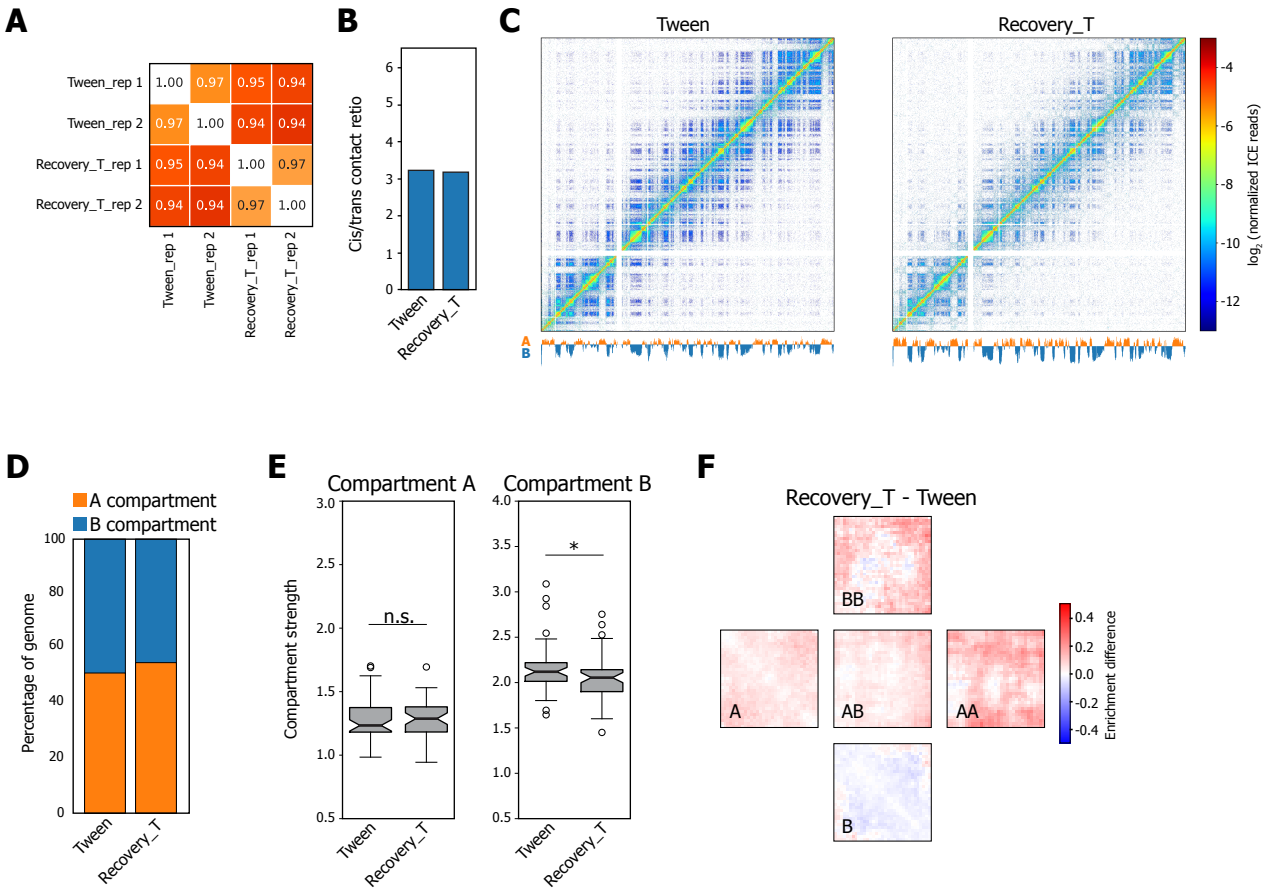

Supplementary Figure S4. Hi-C data processing and compartment annotation in control experiments for Tween permeabilization (Tween-treated HeLa cells). (**A**) Pearson's correlation coefficient between biological replicates of the Hi-C experiments for cells treated with Tween 20 ("Tween") and incubated in a fresh growth media after permeabilization for 1.5 h ("Recovery_T"). (**B**) Ratio between cis (intrachromosomal) and trans (interchromosomal) contacts. (**C**) Visualization of Hi-C contact matrices at a 100-kb resolution. (**D**) Coverage of the genome with A and B compartments. (E) Compartment strength in cis. *$P < 0.05$, n.s., non-significant difference in a Mann-Whitney U-test. (**F**) Pairwise subtraction Recovery_T and Tween pentads.

Supplementary Figure S5

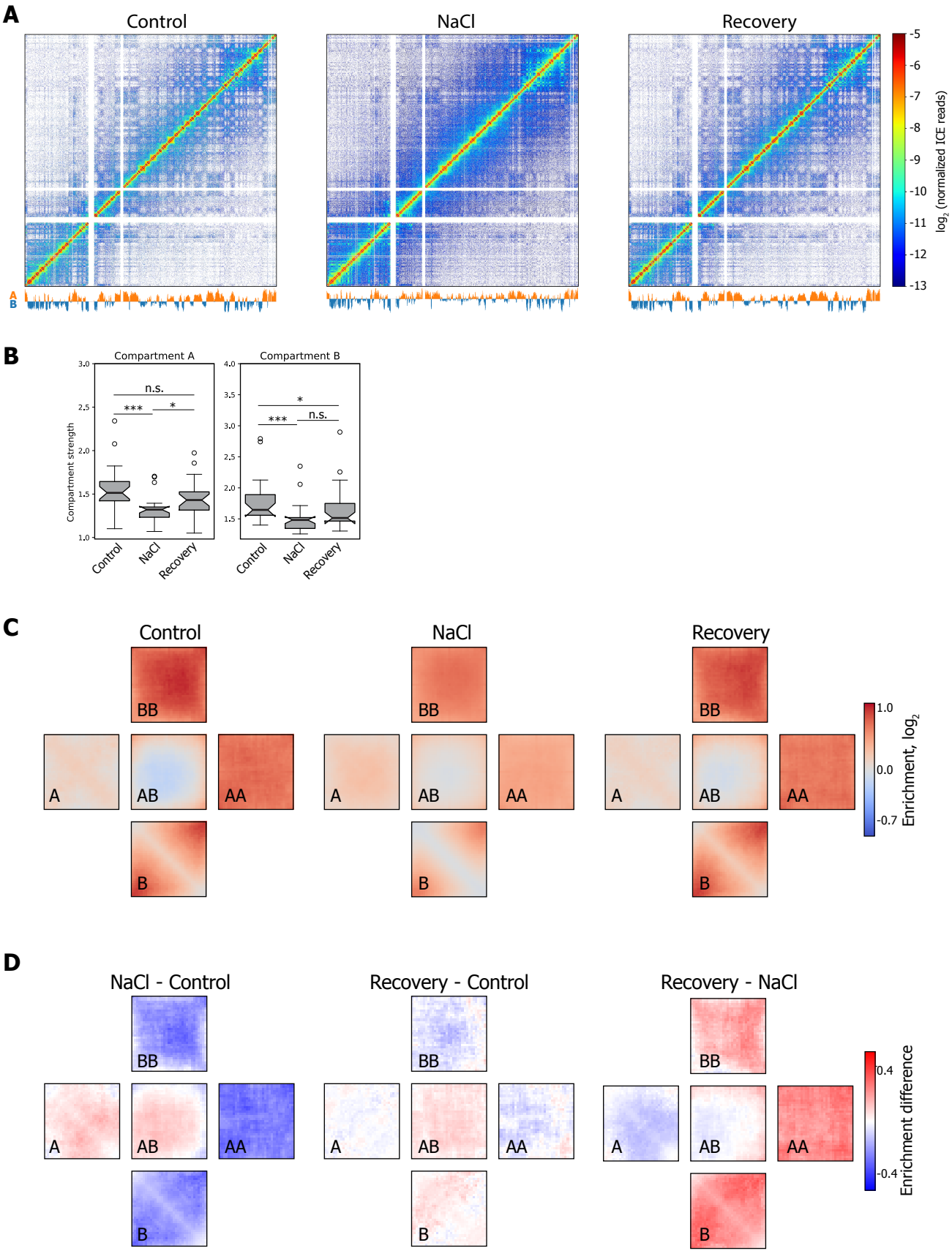

Supplementary Figure S5. Reanalysis of the Hi-C data reported by Amat et al. (**A**) Examples of Hi-C matrices visualized at a 100-kb resolution. (**B**) Compartment strength in control cells, after hyperosmotic shock (NaCl), and after recovery. ***$P < 0.001$, n.s. – non-significant difference in a Mann-Whitney U-test. (**C**) Plots (pentads) showing the observed over the expected contact frequencies inside the A and B compartments at short and large genomic distances and between compartments. (**D**) Pairwise subtractions of Control, NaCl, and Recovery pentads.

Supplementary Figure S6

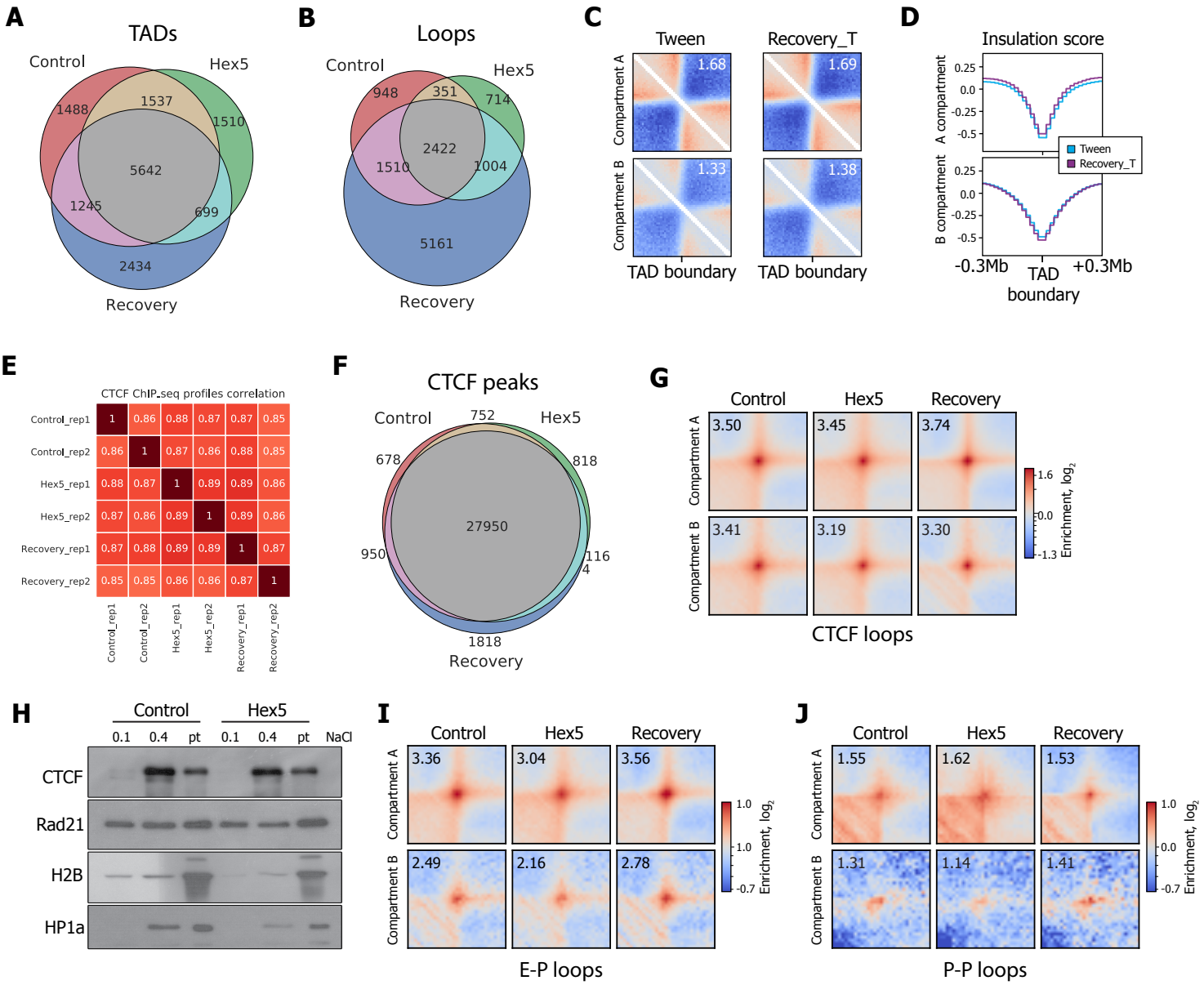

Supplementary Figure S6. (**A**) Venn diagram showing overlapping of TAD boundaries identified in the Control, Hex5, and Recovery samples. (**B**) Venn diagram showing overlapping of loop anchors identified in the Control, Hex5, and Recovery samples. (**C**) Average TAD boundary for the Tween and Recovery_T samples. Number in the upper-right corner shows the boundary strength calculated as the mean value of the average intra-TAD interactions (upper-left and bottom-right quarters) divided by the mean value of average inter-TAD interactions (upper-right quarter). (**D**) Averaged insulation score profile around TAD boundaries (±0.3 Mb). (**E**) Pearson's correlation coefficient between biological replicates of the ChIP-seq experiments. (**F**) Venn diagram showing overlapping CTCF peak sets identified in the Control, Hex5, and Recovery samples. (**G**) Average CTCF-mediated loop in A and B compartments. Number in the upper-left corner shows the enrichment of contacts inside the loop pixel over the background. (**H**) Western blot analysis of CTCF, Rad21, HP1α and histone H2B in different chromatin fractions from control and 1,6-HD-treated HeLa cells prepared by sequential extraction with 0.1 and 0.4 M NaCl. Pellet (Pt): insoluble chromatin fraction. (**I**) Average enhancer-promoter loop in A and B compartments. Number in the upper-left corner shows the enrichment of contacts inside the loop pixel over the background. (**J**) Average promoter-promoter loop in A and B compartments. Number in the upper-left corner shows the enrichment of contacts inside the loop pixel over the background.

Supplementary Table S1. Statistics of the Hi-C data processing.

Replica	Initial reads	Total DS+SS reads	Total DS reads	Same fragment: Total	Same fragment: Self-circles	Same fragment: Dangling ends	Extra Dangling Ends	Valid Pairs	Duplicates	Too Large or Small fragments	Overrepresented fragments	Reads after all filters	cis Reads	trans Reads
Control	437 253 878	396 000 932	298 985 842	15 988 723	1 451 671	6 951 642	42 001 042	240 996 077	52 675 537	18 735 110	11 308 550	158 276 880	134 205 654	24 071 226
Control_rep1	235 131 545	212 458 103	160 256 927	9 845 610	803 259	5 060 999	26 917 815	123 493 502	32 249 934	11 187 909	5 051 705	75 003 954	63 036 500	11 967 454
Control_rep2	202 122 333	183 542 829	138 728 915	6 143 113	648 412	1 890 643	15 083 227	117 502 575	20 301 091	7 578 165	6 266 520	83 356 799	71 242 615	12 114 184
Hex5	422 360 671	383 381 051	288 444 606	15 772 555	1 578 045	3 885 896	27 882 137	244 789 914	52 204 724	11 358 061	13 471 273	167 755 856	142 643 957	25 111 899
Hex5_rep1	209 779 792	189 480 973	141 845 962	8 855 152	772 540	2 422 002	14 660 325	118 330 485	29 392 236	5 669 991	6 496 634	76 771 624	64 383 842	12 387 782
Hex5_rep2	212 580 879	193 900 078	146 598 644	6 917 403	805 505	1 463 894	13 221 812	126 459 429	22 641 441	5 709 861	6 957 911	91 150 216	78 401 532	12 748 684
Recovery	463 832 161	429 271 105	326 810 978	15 989 379	1 558 099	6 814 189	47 074 600	263 746 999	44 265 708	15 451 322	10 471 612	193 558 357	132 242 037	61 316 320
Recovery_rep1	224 845 841	207 680 580	158 016 235	7 185 134	778 161	2 766 436	20 508 097	130 323 004	21 890 163	7 675 042	5 285 969	95 471 830	68 513 580	26 958 250
Recovery_rep2	238 986 320	221 590 525	168 794 743	8 804 245	779 938	4 047 753	26 566 503	133 423 995	22 292 486	7 786 490	5 277 518	98 067 501	63 716 691	34 350 810
Tween	99 413 752	89 619 529	67 850 585	3 947 261	132 152	3 594 334	13 506 158	50 397 166	3 623 895	3 891 810	2 347 932	40 533 529	30 903 988	9 629 541
Tween_rep1	53 484 070	48 134 790	36 350 323	2 233 175	69 577	2 044 708	7 354 117	26 763 031	1 880 438	2 084 189	1 211 751	21 586 653	16 205 842	5 380 811
Tween_rep2	45 929 682	41 484 739	31 500 262	1 714 086	62 575	1 549 626	6 152 041	23 634 135	1 741 382	1 807 858	1 060 423	19 024 472	14 760 864	4 263 608
Recovery_T	81 741 958	74 636 017	56 508 854	2 950 556	107 809	2 675 251	10 082 000	43 476 298	3 226 347	3 211 630	1 667 186	35 371 135	26 919 384	8 451 751
Recovery_T_rep1	43 942 126	40 143 895	30 364 483	1 594 944	64 627	1 440 829	5 153 120	23 616 419	1 641 872	1 710 889	913 980	19 349 678	14 852 196	4 497 482
Recovery_T_rep2	37 799 832	34 492 122	26 144 371	1 355 612	43 182	1 234 422	4 928 880	19 859 879	1 583 525	1 500 865	794 494	15 980 995	12 031 241	3 949 754

Supplementary Table 2. List of publicly available data used in this work.

Data type	Description	URL				
ENCODE ChromHMM, Segway	Combined chromatin state segmentation	http://hgdownload.soe.ucsc.edu/goldenPath/hg19/encodeDCC/wgEncodeAwgSegmentation/wgEncodeAwgSegmentationCombinedHelas3.bed.gz				
ENCODE RNA-seq	PolyA+ RNA-seq, raw reads	https://www.ncbi.nlm.nih.gov/geo/query/acc.cgi?acc=GSE86661				
ENCODE DNase-seq	DNAseI-seq, aligned bam files	http://hgdownload.cse.ucsc.edu/goldenPath/hg19/encodeDCC/wgEncodeOpenChromDnase/				
ENCODE Histone ChIP-seq	ChIP-seq, bigWig and broadPeak files H3K4me1 H3K4me2 H3K4me3 H3K9me3 H3K9ac H3K27me3 H3K27ac H3K36me3 H3K79me2	http://hgdownload.cse.ucsc.edu/goldenPath/hg19/encodeDCC/wgEncodeBroadHistone/				
Amat et. al 2019	Control, Hyperosmotic stress, Recovery	T47D	hg19	Hi-C, RNA-seq	Processed as described in Methods	https://www.ncbi.nlm.nih.gov/geo/query/acc.cgi?acc=GSE111904